Cell Biology International 2002, Vol. 26, No. 3, 279–286
doi:10.1006/cbir.2001.0854, available online at http://www.idealibrary.com on IDEAL®

THE COUPLING OF VINCULIN TO THE CYTOSKELETON IS NOT ESSENTIAL FOR MECHANO-CHEMICAL SIGNALING IN F9 CELLS

WOLFGANG H. GOLDMANN*

Renal Unit, Department of Medicine, Massachusetts General Hospital/Harvard Medical School, Charlestown, MA 02129, U.S.A.

Received 1 May 2001; accepted 12 September 2001

It is well established that mechanical forces can regulate cell growth and guide tissue remodeling, yet little is known about how mechanical signals act at the cell surface membrane to produce biochemical changes in the cell. To explore this question, I used a mouse embryonic F9 vinculin-deficient cell line (γ229), which, unlike wild-type cells, shows no fibronectin-dependent cell spreading. The wild-type cell line exhibited a twofold increase in area over four hours. I observed (i) an earlier rise in intracellular free calcium from ~0.2 to ~3 μM in wild-type compared with γ229 cells, thus similar calcium levels after 4 h; (ii) an initial higher ratio of p-MAP/MAP-Kinase for γ229, but similar FA-Kinase activation; and (iii) a marginal change in intracellular pH $[pH]_i$ in both F9 cell lines. When I applied controlled local stresses directly to integrin receptors using RGD-coated magnetic beads, they displaced to a lesser extent in wild-type than in γ229 cells. Both F9 cell lines showed a small stress-dependent rise in $[Ca^{2+}]_i$ levels and similar PKA-c activity. In summary, the mechanical linkage of integrin-vinculin-cytoskeleton seemed not to be essential for chemical signal transduction.

KEYWORDS: mechano-chemical signaling; vinculin; integrin; cytoskeleton.
ABBREVIATIONS: F9 Vin(−/−); γ229, vinculin-deficient cells; F9Wt, wild-type cells; FN, fibronectin; ECM, extracellular matrix; FAC, focal adhesion complex; CSK, cytoskeleton

INTRODUCTION

Cell spreading on extracellular matrix (ECM) coated substrata has been shown to activate the signaling pathways induced by integrin clustering (Clark and Brugge, 1995; Schwartz *et al.*, 1995; Meredith *et al.*, 1996). These researchers demonstrated that cell binding to ECM, which contains several glycoproteins such as fibronectin (FN), activates the Na^+/H^+ antiporter system resulting in an increase in intracellular pH (Schwartz *et al.*, 1991*a*). Other signaling molecules activated by integrin binding include FA- and MAP-Kinase (Chen *et al.*, 1994; Vuori and Rouslahti, 1993), proteins that mediate inositol lipid turnover (such as phosphatidylinositol kinases, Plopper *et al.*, 1995), and calcium transporters (Schwartz, 1992; Schwartz and Denninghoff, 1994). These studies indicated that ECM interaction with integrin represents a fundamental stimulus for cellular biochemical signaling, and that signals are transmitted to the cell via focal adhesion complexes (FAC) that couple the cell to several actin-associated proteins including talin, vinculin, paxillin, and α-actinin (Burridge *et al.*, 1988), which are critical for anchoring actin microfilament bundles to the plasma membrane.

In this study, I test the hypothesis that the linkage of vinculin between the cell membrane and cytoskeleton, which is required for cell stiffness and lamellipodia formation (Ezzell *et al.*, 1997; Goldmann *et al.*, 1998*a*,*b*) in F9 cells, is also needed for efficient biochemical signal transfer.

Correspondence to: Dr W. H. Goldmann, Massachusetts General Hospital, Renal Unit, Dept. of Medicine, Building 149, 13th Street, Charlestown MA 02129. Fax: 617 726 5671; E-mail: wgoldmann@partners.org
*This work is dedicated to Callum Estevan Santiago on his birthday 30 June 2001.

1065–6995/02/$-see front matter

Using various experimental conditions, intracellular pH and calcium changes, phosphorylation events, and PKA-c levels associated with cell spreading or with controlled local stresses on integrin were monitored.

MATERIALS AND METHODS

Cell culture of F9 embryonic cells

A mouse embryonic F9 carcinoma cell line, in which both vinculin genes were inactivated by homologous recombination (Coll *et al.*, 1995), was a gift from Dr E. D. Adamson, Burnham Institute, La Jolla, CA, U.S.A. The wild-type and F9Vin(−/−) were maintained on 0.1% gelatin-coated charged plastic culture dishes in high glucose (4 g/l) DMEM, 10% calf serum, 20 mM HEPES, 2 mM L-glutamine, and 100 U/ml Penicillin-Streptomycin (Goldmann *et al.*, 1998*a*,*b*). Prior to experiments, the cells were suspended with trypsin, washed in 1% BSA/DMEM and recultured in DMEM containing 4 g/l glucose, 2% calf serum, 2 mM glutamine, 100 U/ml streptomycin, 100 U/ml penicillin.

Measurement of intracellular calcium using Fura-2

In order to measure the relative calcium response, F9 cells were loaded with 5 μM Fura-2 (cf. Product Information Sheet from Molecular Probes, Eugene, OR, U.S.A.) for 30 min at 37°C and then washed in 1% BSA/DMEM. The cells were then placed in a calcium imaging buffer containing 135 mM NaCl, 20 mM HEPES, 5.6 mM glucose, 5 mM KCl, 1 mM $MgSO_4$, 2 mM $CaCl_2$, 3 mM NaH_2PO_4, pH 7.4 with 1% BSA, 10 mg/ml HDL, and 10 mg/ml transferrin. Owing to physical limitations of the CCD camera, the filter wheel attached to the Nikon Diaphot 300 epi-fluorescence microscope, and the computer software, 340 nm and 380 nm images were recorded only every two seconds. Images were then analyzed using VayTek software. To determine the calcium concentration in F9 cells, 340/380 nm ratio imaging was used, i.e. fluorescent digital images were recorded at 340 nm and 380 nm, and the calcium concentration was calculated.

Prior to measuring intracellular calcium levels, I established a system suitable for detecting calcium changes. Using a Nikon Diaphot 300 epi-fluorescence microscope and a *state-of-the-art* VayTek digital imaging system, I first conducted *in vitro* experiments that demonstrated a linear free calcium response when using 5 μM Fura-2 indicator dye in the presence of 10 μM ionomycin. Plotting free calcium against the 340/380 nm fluorescence ratio, a dissociation constant, K_d of 143 nm, which is comparable to published data (Scheenen *et al.*, 1998) was determined.

Measurement of intracellular pH using BCECF

The loading of F9 cells without permeabilization was achieved by incubating them with dilute aqueous dispersions of the cell-permeant BCECF-AM (2′,7′-bis(2-carboxyethyl)-5-(and-6)-carboxy-fluorescein). Once within the cell, non-specific esterases hydrolyzed non-fluorescent BCECF-AM to fluorescent, pH-sensitive BCECF. In brief, approximately 10^5 cells/ml were prepared according to typical procedures. Aliquots of 1 ml BCECF-AM stock solution were diluted 100–500-fold into culture medium in the absence of serum and one volume of aqueous BCECF-AM dispersion to one volume of cell suspension was added. The cells were then incubated for 15–60 min at 37°C and washed twice with fresh medium (cf. Product Information Sheet from Molecular Probes Inc., Eugene, OR, U.S.A.). To equilibrate the intracellular pH with the controlled extracellular medium, *in situ* calibration was performed using the ionophore nigerician (N-1495) at a concentration of 10–50 μM in the presence of 100–150 mM potassium. The ratio of the pH-dependent spectral shift at excitation (490 nm and 440 nm) to that of the fixed emission (535 nm) was used to determine intracellular pH levels.

SDS-PAGE and Western blotting

Cells were lyzed *in situ* on ice for 10 min with 0.2 ml of homogenization buffer that contained 1% Triton X-100, 20 mM sodium phosphate, pH 7.2, 50 mM NaCl, 250 mM sucrose, 2 mM EDTA, and a mixture of protease inhibitors. Equal amounts of proteins from cell extracts were subjected to 10% SDS-PAGE. Resolved proteins were electroblotted at 4°C by applying a constant 100 V for 2 h onto nitrocellulose membranes. Membranes were blocked with 5% BSA in TBS-T (10 mM Tris, pH 7.2, 50 mM NaCl, 0.2% Tween 20) for 1 h at room temperature. The blots were first incubated at 4°C overnight with anti-FAK (1:1000), anti-pMAPK (1:1000), or anti-MAPK (1:1000) monoclonal antibodies in 0.5% BSA, TBS-T. After thorough washing with 0.5% BSA, TBS-T, the membranes were incubated with anti-mouse IgG conjugated with anti-goat IgG (1:5000). The blots

were washed, further developed, and analyzed with an enhanced chemoluminescence (ECL) kit (NEN Life Science Products).

Magnetic bead twisting

The magnetic twisting device used was developed by Wang *et al.* (1993). Controlled mechanical stresses were applied directly to cell surface receptors using ferromagnetic microbeads pre-coated with specific ligands. In brief, beads (4.5 μm; Spherotech) were pre-coated with RGD peptide (Merck or Telios) in a sodium phosphate buffer (0.1 M, pH 5) containing EDAC (1 mg/ml). Following gentle shaking for 2 h at room temperature, the beads were washed twice in PBS and blocked with 1% BSA for at least 1 h prior to use. Adherent cells were allowed to spread for 4 h onto 7 × 22 mm glass coverslips pre-coated with 5 μg/ml fibronectin (Collaborative Research) overnight at 4°C. Beads coated with specific receptor ligands were allowed to bind for 7 min in serum and growth factor free media, and unbound beads were washed off. Bound beads were magnetized horizontally using a 1000 Gauss magnetic field for 10 μs. A 30–50 Gauss vertical magnetic twisting field was applied for 10 min to rotate the beads in place, thereby exerting a rotational shear stress to specific cell surface receptors. This technique can be used to measure cellular responses to applied stress simultaneously by quantifying changes in rotation, i.e. angular strain of the surface bound magnetic beads (Goldmann *et al.*, 2000*a*).

The microscope stage-mounted magnetic bead-twisting device consists of 4 cm diameter Helmholtz coils, which are placed 2.5 cm apart to produce a homogeneous magnetic field. Bright-field images of bound RGD-beads, the same field during application of a vertical twisting field, and digital subtraction of the twisted field from the bound field reveal that not all beads exhibit movement. A purpose-written algorithm is used to calculate the intensity-weighted center of mass of a circular image window with a single bead roughly in the center. As the beads appear black in the image with the surrounding cellular structure nearly white, the image is first inverted. Then, all pixels within the window are set to zero (black) if their intensities are less than the maximum intensity of pixels at the window perimeter. This 'blacking out' ensures that visible structures within the cell do not contribute to the calculated bead position. To measure the accuracy of this method and to compute bead position, the bead motion from multiple consecutive images when no force was present (Alenghat *et al.*, 2000) was analyzed.

Immunofluorescence staining

For PKA-c staining, F9 cells were permeabilized in a cytoskeletal stabilizing buffer (300 mM sucrose, 100 mM NaCl, 3 mM $MgCl_2$, 0.5% Triton X-100, 10 mM PIPES, pH 6.8) containing protease inhibitors (20 μg/ml aprotinin, 1 μg/ml pepstatin, 20 μg/ml leupeptin, 100 μM AEB-SF). The cells were then fixed in ice cold methanol for 7 min and washed in immunofluorescence buffer containing 0.15% Triton X-100, 10% calf serum in PBS and incubated with rabbit anti-PKA-c antibody for 1 h at room temperature. The primary antibody was detected using a Texas Red-labeled donkey anti rabbit IgG secondary antibody (Amersham). Fluorescent images from 15–20 cells/condition were digitally recorded using a DAGE MTI camera and the nuclear staining intensity was quantified using Oncor image analysis software on a Macintosh Quadra 800 computer (Meyer *et al.*, 2000).

Buffers

RIPA buffer: 1% Triton X-100, 1% deoxycholate, 0.1% SDS, 150 mM NaCl, and 50 mM TRIS at pH 7.2. CSK(−) buffer: 10 mM PIPES, 300 mM sucrose, 100 mM NaCl, 3 mM $MgCl_2$, and the addition of the following protease inhibitors: 1 μg/ml pepstatin A, 20 μg/ml leupeptin, 20 μg/ml aprotinin (final), and 1 mM PMSF. CSK(+) buffer: CSK(−) buffer plus 0.5% Triton × 100 (final).

RESULTS

Cell spreading

Previous studies using F9 cells suggest that vinculin is necessary for the mechanical linkage of FAC (Goldmann *et al.*, 1995; Goldmann *et al.*, 1996*a*,*b*; Goldmann *et al.*, 2000*b*). To determine the influence of vinculin coupling with the cytoskeleton and integrin on the spreading behavior of F9 cells, I used different FN concentrations. Over a period of four hours wild-type F9 cells spread at a higher rate on 20 μg/ml FN-coated 35 mm dishes (Fig. 1B) than on 5 μg/ml FN (Fig. 1A); thus the rate of vinculin-deficient cells remained the same at both FN concentrations. The relative area increase was twofold for wild-type cells compared with vinculin-deficient cells at 20 μg/ml FN (Fig. 1B). These observations indicate that the linkage of vinculin

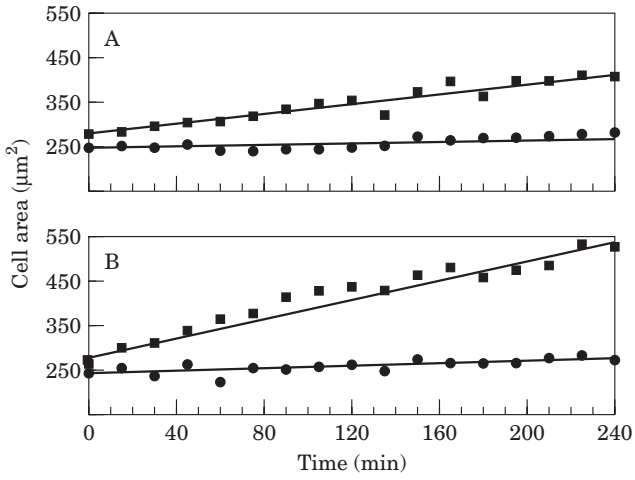

Fig. 1. Spreading of approximately 1×10^{-5} F9Wt (■) and γ229 (●) cells plated in 35 mm dishes coated with 5 μg/ml (A) and 20 μg/ml (B) FN using phase time-lapse video microscopy. The area (μm²) was determined using NIH Image 1.54 program. Buffer: DMEM containing 4 g/l glucose, 2% calf serum, 2 mM glutamine, 100 U/ml streptomycin, 100 U/ml penicillin, 37°C, pH 7.4.

with the cytoskeleton and integrin is necessary for proper spreading, and as also recently shown, for lamellipodia formation (Goldmann and Ingber, 2002). An important question that results from this is whether the lack of vinculin—i.e. the absence of a link between integrin and the cytoskeleton in F9 cells—is purely mechanical or if it also has biochemical implications.

In the first set of experiments, I explored whether F9Wt and F9Vin(−/−) cells are capable of eliciting different calcium responses upon spreading on high FN. Using fluorescence ratio imaging at 340/380 nm, it was found that the K_d in F9 cells plated on 20 μg/ml FN was ~0.5 μM (Fig. 2, inset). Observing calcium changes after plating for 240 min, I detected an increase ranging from ~0.2 to ~3 μM free $[Ca^{2+}]_i$ for both cell lines. As shown in Fig. 2, both cell lines exhibited a similar increase for 30 min and thereafter wild-type cells showed a faster increase than vinculin-deficient cells. Thus, both cell lines reach similar free $[Ca^{2+}]_i$ concentrations after four hours of spreading. This result indicates that the mechanical linkage of vinculin in F9 cells is probably not required for calcium signaling; and other factors may also be responsible for the delayed increase of free $[Ca^{2+}]_i$ in F9Vin(−/−) cells.

Utilizing the Nikon Diaphot 300 microscope and the VayTek digital imaging system, the intracellular pH in F9 cells was also measured. Loading cells with the pH sensitive dye BCECF using the proton ionophore nigericin, a linear relation between pH 6.5 and 9 and projected area was observed. Plotting pH changes calculated from fluorescence ratios at 490/440 nm and 240 min after plating

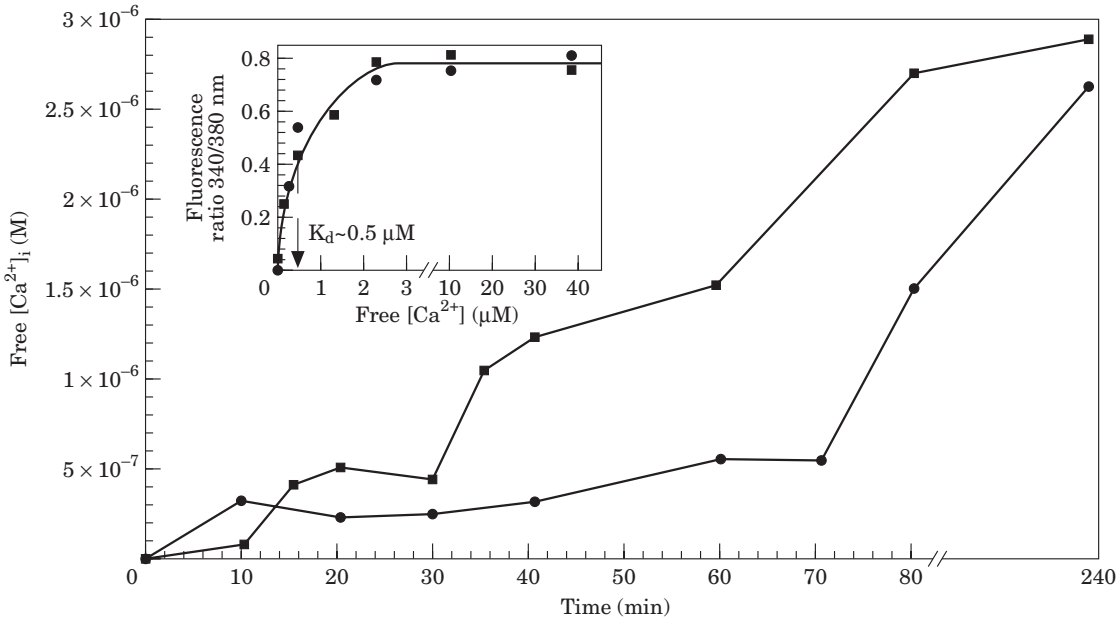

Fig. 2. Plot of free $[Ca^{2+}]_i$ in F9 cells with time. Approximately 1×10^{-5} F9Wt (■) and γ229 (●) cells were plated in 35 mm dishes coated with 20 μg/ml FN. Both F9 cell lines show an increase in intracellular free calcium between ~0.2 to ~3 μM with time. *Inset*: determination of dissociation constant, K_d (~0.5 μM Ca^{2+}) for both F9 cell lines. An increase in fluorescent ratio at 340/380 nm was observed with increasing concentrations of free intracellular calcium. Conditions: F9 cells are loaded with 5 μM Fura-2 for 30 min prior to experimentation according to the protocol in Materials and Methods.

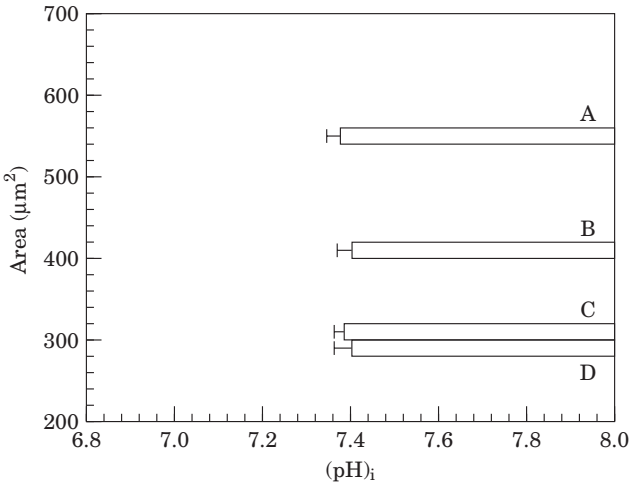

Fig. 3. Spreading of approximately 1×10^{-5} F9Wt and γ229 cells plated in 35 mm dishes coated with 20 μg/ml (A,C) and 5 μg/ml (B,D) FN, respectively. Changes (pH)i were recorded at 535 nm (emission) after loading the cells with BCECF-AM for 60 min. From the ratio of the excitation wavelengths at 440 nm and 490 nm the intracellular pH was determined, using an equation provided by the supplier. Conditions as described in Materials and Methods.

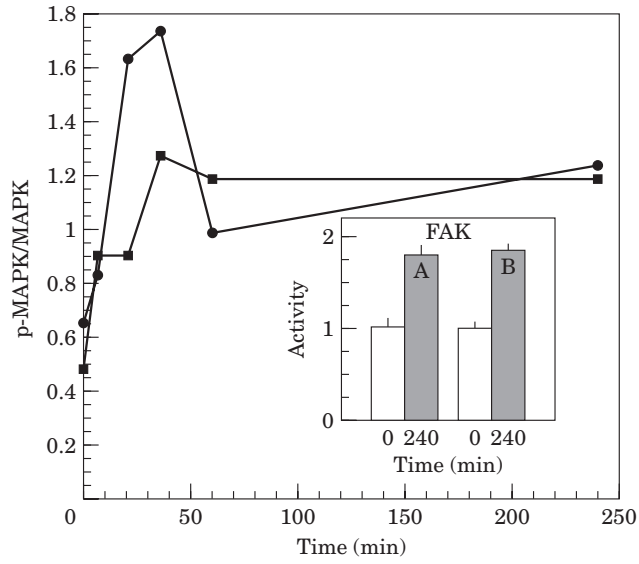

Fig. 4. Ratio of p-MAPK and MAPK measured over 4 h. Approximately 1×10^{-5} F9Wt (■) and γ229 (●) cells were plated in 35 mm dishes coated with 20 μg/ml FN. At various time points the activity of MAP-Kinase and p-MAP-Kinase was determined using SDS-PAGE and Western blots. The ratio of p-MAP/MAP-Kinase was plotted over time and γ229 cells showed an earlier and higher peak (~30 min); thus after 240 min this was similar for both F9 cell lines (approx. twofold increase). *Inset*: FA-Kinase activity also increased twofold over 4 h. (A) F9Wt and (B) ξ229 cells. Buffer conditions as described in Materials and Methods.

wild-type and γ229 cells on high (Fig. 3A+C) and low FN (Fig. 3B+D), I detected only minor changes related to the cell spreading area in both cell lines. This result indicates that integrin-mediated changes in intracellular pH do not need the physical presence of vinculin to signal biochemical events.

Further, phosphorylation of FA- and MAP-Kinase, both of which have been reported to be activated specifically upon cell spreading on the ECM, were studied (Davis *et al.*, 1993). For this purpose, an assay in which approximately 1×10^5 F9 cells are plated on FN-coated 35 mm dishes that have been serum-starved for 24 h prior to experimentation was used. Exposing F9 cells to CSK(−) and CSK(+) buffer for 10 min and then extracting with RIPA-buffer at various times and degrees of spreading, the effect of cell spreading on the phosphorylation activity of FA- and MAP-Kinase in F9 cells. SDS/PAGE and Western blot assays provided information of their phosphorylation upon spreading and possibly which constituents are activated in the signaling process. Antibodies against FA-, MAP-, and p-MAP-Kinase were used as markers for phosphorylation events in response to spreading. Figure 4 shows—using the ratio of p-MAP- and MAP-Kinase—that F9Vin(−/−) cells (●) peak at an earlier time (~30 min after plating on high FN) than F9 wild type cells (■) but reached the same ratio after 240 min, while the FA-Kinase activity increased for both F9 cell lines approximately by a factor of 2 (Fig. 4, inset). This result further indicates that integrin-mediated cell adhesion does not require vinculin to couple with the FAC proteins for mechano-chemical transduction.

Mechanical force application

To address the significance of mechanical force transmission through integrins on two physiological activators, i.e. calcium and PKA-c, I applied a microscope stage-mounted magnetic bead-twisting device that can be used in conjunction with ratio image analysis. This method can help to answer questions regarding the immediate activation of ionic signal generation following mechanical force transmission through integrins; it can also be used to determine whether 'classic' effectors, such as intracellular calcium, become mobilized or to discover other 'unknown' effectors that may play a role in cellular mechanotransduction. Using this method and a purpose-written image analysis program, a simple algorithm gave the bead position on integrin receptors with sub-pixel resolution (Alenghat *et al.*, 2000).

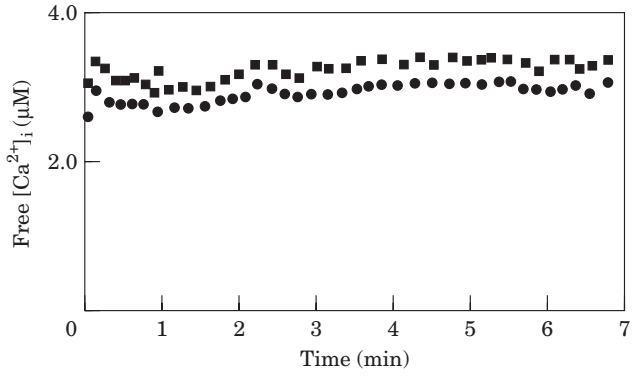

Fig. 5. Free intracellular calcium in F9 cells measured for 7 min after the application of a magnetic twisting force of 50 Gauss. About 1×10^{-5} F9Wt (■) and γ229 (●) cells were attached to high FN-coated 35 mm dishes for 4 h and after the addition of approx. 3×10^4 RGD-coated beads 30 min prior to experimentation, the free $[Ca^{2+}]_i$ was detected by Fura-2 and calculated from ratio imaging at 340/380 nm. Conditions as in Fig. 1.

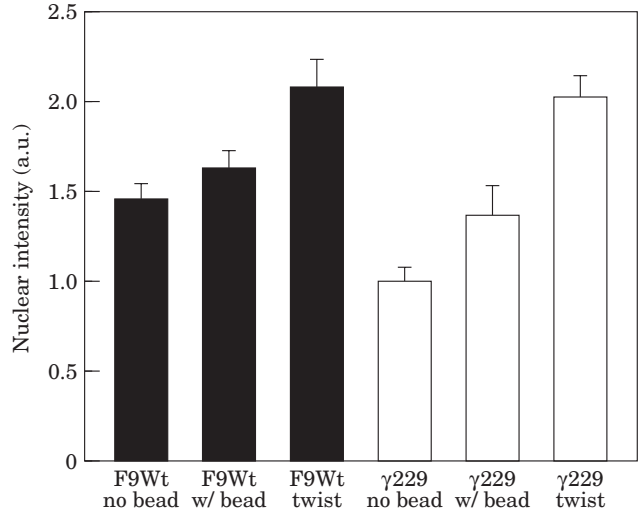

Fig. 6. Magnetic twisting of RGD-coated beads increased the recruitment of the nuclear intensity (PKA-c) of F9Wt and γ229 cells. RGD-coated beads were allowed to bind to F9 cells 5 min (before unbound beads were washed off), followed by application of 15.6 dyne/cm^2 twisting stress for 5 min. No-twist controls were placed at 37°C in parallel to cells subjected to mechanical force application. Error bars indicate S.E.M. of three independent experiments. Conditions as in Fig. 1.

The microscope stage-mounted magnetic bead-twisting device was used to investigate whether any local external forces exerted on the cell membrane—other than spreading—are capable of eliciting a calcium response in F9 cells. In order to view real-time changes in intracellular calcium following application of a rotational shear stress, I applied twisting shear stresses to F9 cells cultured on a 35 mm glass-bottom dish. Results showed only a slight, but detectable, increase in calcium levels that occurred for about 3–5 s after force application (Fig. 5). The stress applied by this method was approximately 100 dyne/cm^2. Furthermore, different stresses (whether undulating or intermittent and at varying strengths) elicited only small changes in intracellular calcium ($\ll 5\%$). To determine whether prolonged force application is capable of producing an increase in intracellular calcium, longer periods were studied. The baseline calcium concentration (no beads) in F9 cells was calculated to be approximately 3 μM, and following RGD-bead binding and twisting, there was little change in intracellular calcium concentration during a 7 min time course (Fig. 5). This finding supports observations that putting stress on integrin receptors of F9 cells after 4 h of cell spreading using RGD-coated beads does not affect intracellular calcium levels.

To determine whether PKA-c becomes activated following mechanical stress application, ligand-coated microbeads were bound to F9 cells with or without the application of a 30 Gauss twisting field, which produces a shear stress of 100 dynes/cm^2. When RGD-beads were bound to wild-type and γ229 cells without force application, about 15–30% increase in total nuclear staining intensity for PKA-c was observed compared to no beads. The bound RGD-beads were then magnetically twisted and compared with no-bead controls (Fig. 6). Results from these experiments show—although wild-type F9 cells have higher initial nuclear intensity levels compared to vinculin-deficient cells—the final intensity after magnetic twisting reaches similar levels for both F9 cells, indicating that vinculin and mechanical coupling between integrin and actin cytoskeleton is probably not required for stress- and integrin-dependent activation of PKA-c signaling in F9 cells. This is consistent with results using EC cells, which suggest that the mechano-chemical transduction mechanism is likely to occur directly at the cell surface (Plopper *et al.*, 1995; Wang *et al.*, 1993; Wang and Ingber, 1994).

DISCUSSION

In this work, I have shown that vinculin-deficient F9 cells spread more slowly and to a lesser degree on various concentrations of FN-coated dishes than do wild-type cells. As previously reported, the lack of spreading is probably due to reduced stress fiber and lamellipodia formation and to decreased mechanical coupling between integrins and the

internal cytoskeleton (Ezzell *et al.*, 1997; Xu *et al.*, 1998; Goldmann and Ingber, 2002). Thus, when vinculin is transfected back into F9Vin(−/−) cells, all the mechanical and viscoelastic properties are restored to near wild-type level (Goldmann *et al.*, 1998*b*). These data strongly suggest that vinculin represents a molecule that mediates mechanical signaling. The question that emerged from these studies was whether or not mechano-chemical transduction requires vinculin-dependent mechanical coupling.

In an attempt to address this question, I investigated the influence of different FN concentrations on the spreading behavior of F9 cells. Since Ingber's laboratory at Children's Hospital, Boston had previously shown that cell binding to ECM and cell spreading activate the Na^+/H^+ antiporter system and increase the Na^+/H^+ exchange to elevate $[Ca^{2+}]_i$ (Schwartz *et al.*, 1991*b*), I investigated this phenomenon comparing wild-type with γ229 cells. An ECM density-dependent increase in both $[Ca^{2+}]_i$ and $[pH]_i$ and changes in $[Ca^{2+}]_i$ that would closely parallel alterations in cell stiffness were expected, since wild-type cells are ∼20% more rigid than γ229 cells (Goldmann *et al.*, 1998*b*). Thus, the spreading experiments showed an intracellular calcium increase and a slight decrease in pH_i for both cell lines. On closer examination, a faster rise of free $[Ca^{2+}]_i$ was observed for wild-type cells than for γ229 cells, which reached similar levels only after 4 h. When these cells were then stimulated by exposing them to RGD-coated microbeads for 20 min and applying controlled external magnetic forces, no further increase in free $[Ca^{2+}]_i$ was observed (unpublished results).

Cell attachment to ECM and integrin binding are also known to activate different classes of chemical signaling pathway that share common downstream targets. This effect can be mediated by clustering of specific cell surface integrin receptors (Schwartz *et al.*, 1991*a*,*b*). Signaling molecules that have been shown to be activated specifically by adhesion, ECM, and integrin binding include MAP-Kinase, intracellular calcium stores, and Na^+/H^+ antiporter (Davis *et al.*, 1993). The signals from the ECM appear rapidly, i.e. Na^+/H^+ antiporter within 10 min and phosphorylation within 20 min. In cell spreading experiments, F9 cells showed an increase in MAP-Kinase activation and intracellular calcium, and a slight decrease in pH_i upon spreading. However, on closer examination, wild-type cells showed an initial higher free $[Ca^{2+}]_i$ and a lower phosphorylation level of MAP-Kinase activity, which are the same for both cell lines after 4 h. Upon force application using magnetometry, there were no detectable significant differences in intracellular calcium or PKA-c activity between F9 cell lines, indicating that vinculin is probably not needed for these signaling events.

To date, only a sparse literature exists to support direct protein–protein interaction within the transmembrane or cytoplasmic domains of integrin (Meyer *et al.*, 2000), yet data in this study show that it must be activated, either directly or indirectly, by mechanical force application to integrin. Since there were signaling responses of downstream effectors (PKA-c), and the disruption of an intact FAC (i.e. the absence of vinculin and any connection between integrin and the internal cytoskeleton) did not alter signal propagation, activation of this signaling pathway must be localized near the site of mechanical force transfer. In all, the findings are supportive of the idea that the link between vinculin-integrin-cytoskeleton is not a pre-requisite for biochemical signaling in F9 cells; however, more detailed studies are needed to understand the complex function of vinculin with regard to the *rac* signaling pathway that drives lamellipodia extension (Goldmann & Ingber, 2002).

ACKNOWLEDGEMENTS

I would like to acknowledge Drs Jose-Luis Alonso, Robert Mannix, Ben Fabry, and Tom Polte for their help and Judith Feldmann, PhD for careful reading and editing of the manuscript. This work was supported by a *grant-in-aid* from the German government and NATO.

REFERENCES

Alenghat FJ, Fabry B, Tsai KY, Goldmann WH, Ingber DE, 2000. Analysis of cell mechanics in single vinculin-deficient cells using a magnetic tweezer. *Biochem Biophys Res Commun* **277:** 93–99.

Burridge K, Fath K, Kelly T, Nukolls G, Turner C, 1988. Focal adhesion: transmembrane junctions between the extracellular matrix and the cytoskeleton. *Annu Rev Cell Biol* **4:** 17–78.

Chen Q, Kinch M, Lin T, Burridge K, Juliano R, 1994. Integrin-mediated cell adhesion activates mitogen-activated protein kinases. *J Biol Chem* **269:** 26602–26605.

Clark EA, Brugge JS, 1995. Integrins and signal transduction pathways: the road taken. *Science* **268:** 233–239.

Coll JL, Ben-Ze'ev A, Ezzell RM, Rodriguez Fernandez JL, Baribault H, Oshima TG, Adamson ED, 1995. Targeted disruption of the vinculin gene in F9 and ES cells changes cell morphology, adhesion and locomotion. *Proc Nat Acad Sci USA* **92:** 9161–9165.

Davis E, 1993. Intracellular and intercellular signals and their transduction via the plasma membrane-cytoskeleton interface. *Sem Cell Biol* **4:** 139–147.

Ezzell RM, Goldmann WH, Wang N, Parasharama N, Ingber DE, 1997. Vinculin promotes cell spreading by mechanically coupling integrins to the cytoskeleton. *Exp Cell Res* **231:** 14–26.

Goldmann WH, Schindl M, Cardozo TJ, Ezzell RM, 1995. Motility of vinculin-deficient F9 embryonic carcinoma cells analyzed by video, laser confocal, and reflection interference contrast microscopy. *Exp Cell Res* **221:** 311–319.

Goldmann WH, Ezzell RM, Adamson ED, Niggli V, Isenberg G, 1996*a*. Vinculin, talin and focal adhesions. *J Muscle Res Cell Motil* **17:** 1–5.

Goldmann WH, Ezzell RM, 1996*b*. Viscoelasticity in wild-type and vinculin-deficient (5.51) mouse embryonic carcinoma cells examined by atomic force microscopy and rheology. *Exp Cell Res* **226:** 234–236.

Goldmann WH, Galneder R, Ludwig M, Kromm A, Ezzell RM, 1998*a*. Differences in F9 and 5.51 cell elasticity determined by cell poking and atomic force microscopy. *FEBS Lett* **424:** 139–142.

Goldmann WH, Galneder R, Ludwig M, Xu W, Adamson ED, Wang N, Ezzell RM, 1998*b*. Differences in elasticity of vinculin-deficient F9 cells measured by magnetometry and atomic force microscopy. *Exp Cell Res* **239:** 235–242.

Goldmann WH, Alonso JL, Bojanowski K, *et al.*, 2000*a*. In: Carraway KL, Carraway CAC, eds. *Cytoskeleton: Signaling and Cell Regulation*. Oxford, Oxford University Press. 245–276.

Goldmann WH, 2000*b*. Mechanical manipulation of animal cells: cell indentation. *Biotechn Lett* **22:** 431–435.

Goldmann WH, Ingber DE, 2002. Intact vinculin protein is required for control of cell shape, cell mechanics, and rac-dependant lamellipodia formation. *Biochem Biophys Res Comm* **290:** 749–755.

Meredith JE Jr, Winitz S, Lewis JM, Hess S, Ren XD, Renshaw MW, Schwartz MA, 1996. The regulation of growth and intracellular signaling by integrins. *Endocrine Rev* **17:** 207–220.

Meyer CJ, Alenghat FJ, Rim P, Fong JH, Fabry B, Ingber DE, 2000. Mechanical control of cyclic AMP signalling and gene transcription through integrins. *Nat Cell Biol* **9:** 666–668.

Plopper GE, McNamee HP, Dike LE, Bojanowski K, Ingber DE, 1995. Convergence of integrin and growth factor receptor signaling pathways within the focal adhesion complex. *Mol Biol Cell* **6:** 1349–1365.

Scheenen WJJM, Hofer AM, Pozzan T, 1998. Intracellular measurement of calcium using fluorescent probes. In: *Cell Biology: A Laboratory Handbook*, 2nd Edition, Vol. 3. Academic Press.

Schwartz MA, Ingber DE, Lawrence M, Springer TA, Lechene C, 1991*a*. Multiple integrins share the ability to induce elevation of intracellular pH. *Exp Cell Res* **195:** 533–535.

Schwartz MA, Lechene C, Ingber DE, 1991*b*. Insoluble fibronectin activates the Na^+/H^+ antiporter by clustering and immunobilizing integrin alpha 5 beta 1, independent of cell shape. *Proc Natl Acad Sci USA* **88:** 7849–7853.

Schwartz MA, 1992. Spreading of human endothelial cells on fibronectin or vitronectin triggers elevation of intracellular free calcium. *J Cell Biol* **120:** 1003–1010.

Schwartz MA, Denninghoff K, 1994. Alpha v integrins mediate the rise in intracellular calcium in endothelial cells on fibronectin even though they play a minor role in adhesion. *J Biol Chem* **269:** 11133–11137.

Schwartz MA, Schaller MD, Ginsberg MH, 1995. Integrins: emerging paradigms of signal transduction. *Annu Rev Cell Dev Biol* **11:** 549–599.

Vuori K, Rouslahti E, 1993. Activation of protein kinase C precedes alpha5beta1 integrin mediated cell spreading on fibronectin. *J Biol Chem* **268:** 21459–21462.

Wang N, Butler JP, Ingber DE, 1993. Mechanotransduction across the cell surface and through the cytoskeleton. *Science* **260:** 1124–1127.

Wang N, Ingber DE, 1994. Control of cytoskeletal mechanics by extracellular matrix, cell shape, and mechanical tension. *Biophys J* **66:** 2181–2189.

Xu W, Coll JL, Adamson ED, 1998. Rescue of the mutant phenotype by reexpression of full-length vinculin in null F9 cells; effects on cell locomotion by domain deleted vinculin. *J Cell Sci* **111:** 1535–1544.